



Concentration dependent hydrogen diffusion in tungsten



T. Ahlgren*, L. Bukonte

Accelerator Laboratory, University of Helsinki, P.O. Box 43, 00014, Finland

H I G H L I G H T S

- The recommended value of 0.39 eV for the H in W migration barrier should be changed to 0.25 eV.
- The random oscillation of atoms around the equilibrium position can be dealt with in diffusion simulations.
- Hydrogen diffusion in tungsten is highly concentration dependent.

A R T I C L E I N F O

Article history:

Received 24 November 2015

Received in revised form

19 April 2016

Accepted 26 June 2016

Available online 29 June 2016

A B S T R A C T

The diffusion of hydrogen in tungsten is studied as a function of temperature, hydrogen concentration and pressure using Molecular Dynamics technique. A new analysis method to determine diffusion coefficients that accounts for the random oscillation of atoms around the equilibrium position is presented. The results indicate that the hydrogen migration barrier of 0.25 eV should be used instead of the presently recommended value of 0.39 eV. This conclusion is supported by both experiments and density functional theory calculations. Moreover, the migration volume at the saddle point for H in W is found to be positive: $\Delta V_m \approx 0.488 \text{ \AA}^3$, leading to a decrease in the diffusivity at high pressures. At high H concentrations, a dramatic reduction in the diffusion coefficient is observed, due to site blocking and the repulsive H-H interaction. The results of this study indicates that high flux hydrogen irradiation leads to much higher H concentrations in tungsten than expected.

© 2016 Elsevier B.V. All rights reserved.

1. Introduction

Tungsten (W) is one of the strongest candidates to be used as the divertor plate material for the next step fusion device (ITER) due to its high melting point, low erosion rate, good thermal conductivity and low hydrogen retention. Such combination of properties makes W a promising plasma-facing wall material. However, continuous bombardment with low energy hydrogen isotopes is seen to introduce defects in plasma facing materials. Open volume defects, such as vacancies, are known to trap hydrogen (H) and thus are the main reasons for H retention in W. In fusion reactors this is a critical issue due to the tritium retention.

The presence of H strongly affects most of the W properties, due to phenomena like vacancy formation and blistering [1,2]. Moreover, H is known to be trapped in impurities, vacancies, dislocations and grain boundaries [3–5], affecting the micro-structure evolution

of the material. In order to be able to predict and calculate the evolution of the micro-structure, tritium retention, and other thermal and mechanical properties, it is essential to know the H concentration present in the material.

The H atom is an endothermic impurity in W with a solution energy E_{sol} of about 1 eV [6]. This means that the equilibrium H concentration $C_{H,eq}$ in W is very low unless a large H_2 pressure (P) is present at the W surface at high temperature (T); $C_{H,eq} \propto \sqrt{P} \exp(-(E_{sol} - T\Delta S)/k_B T)$, where ΔS is the entropy change and k_B is the Boltzmann constant. However, large H flux from a fusion device, plasma source or ion implanter can result in concentrations that considerably exceeds equilibrium value in W. This H concentration is proportional to the incoming flux and inverse proportional to the H diffusivity. The H diffusivity, however, is a function of the concentration itself. At high concentrations, the diffusivity should decrease due to the adjacent interstitial site blocking [7], and due to the short-range H-H repulsion [8,9]. Hence, the decreasing diffusivity will increase the

* Corresponding author. Pietari Kalminkatu 2, P.O. Box 43, 00014, Finland.
E-mail address: tommy.ahlgren@helsinki.fi (T. Ahlgren).

concentration, affecting the properties of the W material. To our knowledge, no data on concentration dependent H diffusion in W is found in the literature.

In this study, using molecular dynamics simulations we derive equations showing H diffusion coefficient dependence on the H concentration. We present a new analysis method to determine diffusion coefficients that accounts for the random oscillation of atoms around the equilibrium position. Moreover, we review the H diffusion coefficient at low concentrations in W, and suggest that the commonly used H diffusion parameters should be revised.

2. Computational method

Our modelling of H diffusion in W is done employing molecular dynamics simulations (MD) [10] using the bond-order potential by Li et al. [11] to describe the forces between W-W, W-H and H-H atoms. We use the Berendsen thermostat to control the atom velocity distribution, which for large systems of over hundreds of atoms approximately generates a correct canonical ensemble. Since the timestep is proportional to $M^{-1/2}$ [10], where M is the atom mass, heavy hydrogen isotope deuterium (D) is chosen to improve the efficiency of MD simulations. The results are easily scaled with square the root of the atomic mass of D to obtain the diffusion coefficient of H [12,13].

Depending on the D concentration two different W simulation cell sizes are used. For high D concentrations we use a $6 \times 6 \times 6$, 432 W atom system. We have checked the validity of the $6 \times 6 \times 6$ system size by performing the simulations in the low limit D concentration case (1 D atom in the system) also with a $10 \times 10 \times 10$ cell containing 2000 W atoms. The system size does not affect the resulting diffusion coefficients. To track the actual D position during the MD simulations, also positions omitting the periodic boundary conditions were saved. The pressure during simulation is kept constant at 0 kbar. Temperatures lower than 300 K are not investigated due to the limitations of the MD simulation time scale, besides, at T below 300 K quantum tunneling starts to dominate [14,15].

To determine the diffusion coefficient, we need the atomic positions at different simulation times. How often the positions can be saved is bounded by the data storage capacity. However, if the positions are saved too seldom, the error in calculating the diffusion coefficient increases, see section 3. To optimize the simulations, we counted the number of atomic diffusion jumps as a function of the saving time interval. The 3D diffusion coefficient in cubic lattices can be written as: $D = 1/6 \cdot \lambda^2 \cdot \Gamma$, where λ is the diffusion jump length and Γ is the jump frequency. The mean residence time the diffusing atom spends at each site becomes: $T_{res} = 1/\Gamma = \lambda^2/(6D)$. In Table 1 we see that saving the position about hundred times more often than the mean time between diffusion jumps ($0.01 T_{res}$), as is done in this study, records about 99.2% of all the diffusion jumps.

Table 1

The percentage of the counted atomic diffusion jumps in the simulation as a function of the saving time interval.

Times Δ saving time (T_{res})	Number of jumps saved
1000	0.01%
100	1.00%
10	9.66%
1	58.45%
0.1	94.04%
0.01	99.19%

3. Results and discussion

3.1. Diffusion coefficient at low concentrations

The simulation of D diffusion coefficient for low D concentration ($D/W = 1/2000$) is done in the temperature range between 300 and 1500 K, and diffusion times between 1 and 20 ns. The D position during simulation is tracked using the Wigner-Seitz cell analysis, where the closest tetrahedral interstitial site (TIS) is found and is assigned to be the D position in the diffusion coefficient analysis. Fig. 1 illustrates the real X-position of the D atom, and the one used in the analysis as a function of the simulation time. The deuterium diffusion coefficient is determined by the Einstein-Smoluchowsky equation using the independent interval method (IIM) [16], as follows:

$$D = \frac{1}{6N} \frac{\sum_i^N \Delta R_i^2}{\sum_i^N \Delta T_i}, \quad (1)$$

where ΔR_i^2 is the square displacement of the diffusing atom, ΔT_i – the diffusion time and N – the number of intervals the path is divided into. The diffusion coefficient can further be written as the Arrhenius function of the pre-exponential factor D_0 and migration barrier E_m

$$D = D_0 \exp\left(-\frac{E_m}{k_B T}\right), \quad (2)$$

where T is the absolute temperature and k_B the Boltzmann constant. The diffusion parameters from this study and found in the literature are presented in Table 2.

The currently accepted and recommended [20] migration barrier of 0.39 eV for hydrogen is from Fraunfelder experiments [6]. Table 2 and Fig. 2 show that if the Arrhenius fit to Fraunfelder data is done omitting the two lowest temperature points (less than 1400 K), the migration barrier results in value of 0.25 eV. This value is consistent with the present study, the DFT study by Heinola et al. [18] and the experimental permeation study by Nemanic et al. [19]. The Fraunfelder data has been divided by the square root of the D atomic mass to account for the isotope effect on diffusion pre-exponential factor [12,13].

The two lowest temperature Fraunfelder diffusion coefficients

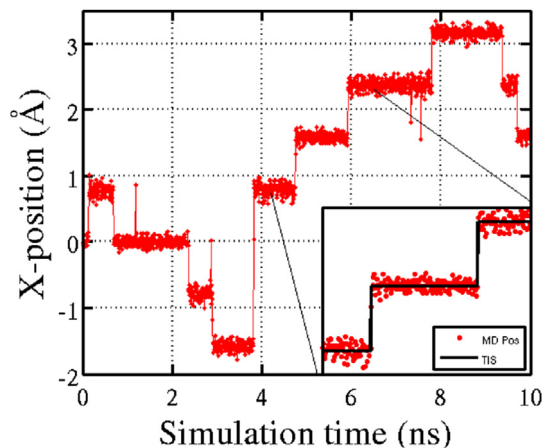


Fig. 1. Example of the D atom X-position during the 300 K MD simulation. The random oscillation around the tetrahedral interstitial site (TIS) is eliminated using the Wigner-Seitz cell analysis, giving a more accurate diffusion coefficient.

Table 2

Deuterium diffusion pre-exponential factors (D_0), migration barriers (E_m) and diffusion coefficients at 300 K in W. The Fraunfelder and Grigorev et al. [17] data have been divided by square root of two to convert H to D parameters.

	D_0 (m ² /s)	E_m (eV)	D (300 K) (m ² /s)
Exp [6] whole data set	2.73×10^{-7}	0.39	8×10^{-14}
Exp [6] two points removed ^a	1.12×10^{-7}	0.25	7×10^{-12}
MD (present study)	$(0.88 \pm 0.05) \times 10^{-7}$	(0.25 ± 0.01)	6×10^{-12}
MD [17]	9.33×10^{-9}	0.23	2×10^{-12}
DFT [18]	0.48×10^{-7}	0.26	2×10^{-12}
DFT [9]	–	0.20	–
DFT [24] ^b	–	0.38	–
Exp [19]	–	0.27	–

^a Two lowest temperature points removed, see text.

^b Zero point energy corrected value.

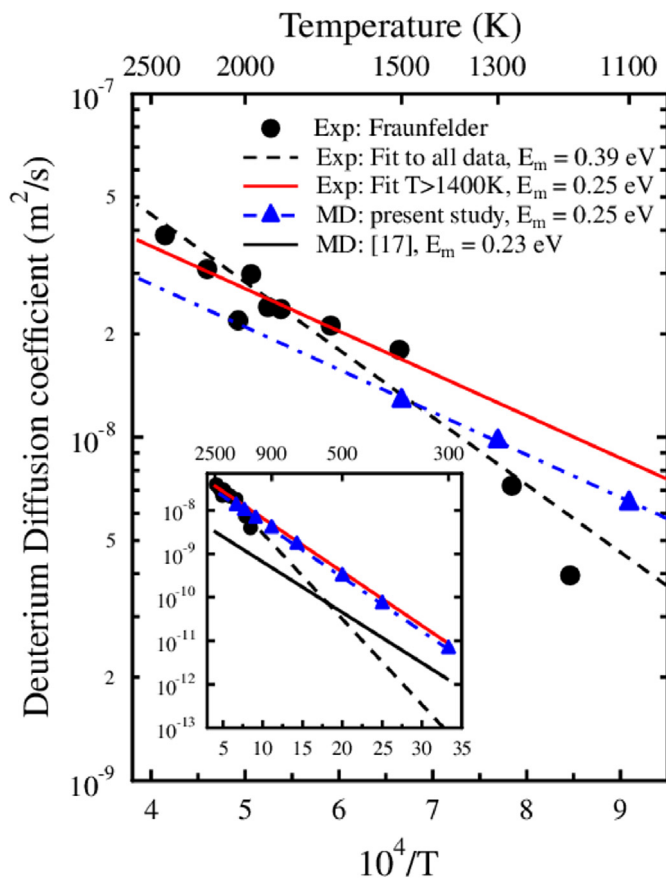


Fig. 2. Arrhenius plot of simulated and experimental D diffusion coefficients. The Fraunfelder data has been divided by square root of two, see text. The red line is the fit to Fraunfelder data where the two lowest temperature points, $T < 1400$ K, have been omitted. The labels and units in the inset are the same as for the main plot. (For interpretation of the references to colour in this figure legend, the reader is referred to the web version of this article.)

are suggested to be too low due to trapping effects [3]; if the diffusing atom is occasionally trapped during the experiment, the apparent diffusion coefficient will be lower than it actually is without trapping. The change in the migration barrier from 0.39 eV to 0.25 eV has an enormous effect on the diffusion coefficients close to room temperature, as seen in Table 2 where the 300 K diffusion coefficient for 0.39 eV is more than two orders of magnitude

smaller than for 0.25 eV.

The MD diffusion data by Grigorev et al. [17] shown in Table 2 and Fig. 2, has a migration barrier of 0.23 eV, but a much lower pre-exponential factor than obtained in this study. This is very typical for MD results which depend on the potentials used and how the potential fits are done. The difference in the migration barriers obtained by DFT, 0.26 eV, Heinola et al. [18] and 0.2 eV, Liu et al. [9] has at least two reasons: firstly, in the study by Heinola et al. the nearest W atoms were not allowed to relax in the nudged elastic band calculations during the D jump from one TIS to another. This course of action is justified because the heavy W atoms do not have time to relax their positions during the very short time it takes for the light D atom to make a jump. The second reason for discrepancy might be the drag method used by Liu et al. which is known to often miss the actual saddle point [23,24]. The relatively high DFT migration barrier 0.38 eV obtained by Johnson et al. [24], Table 2 is surprising. The reason for this is not clear, but it might be due to a smaller simulation cell than the one used in Ref. [18]. In a small simulation cell with periodic boundary conditions, the jumping D atom will interact with its own image in a neighboring cell. In section 3.3 it is shown that the migration barrier increases when the D atom concentration increases.

In the review paper by Tanabe [21], results of several H diffusion studies in W are presented. A large variation in H migration barrier is observed, ranging between 0.12 and 2.0 eV. The conclusion by Tanabe, supported by results obtained with tritium tracer technique (TTT) [22], is that the Fraunfelders' migration barrier of 0.39 eV is still the most reliable one. However, present manufacturing methods to produce W are such that defects and impurities are always found in the material. For instance, in the powder metallurgy process, a binder is used, which leaves C and O impurities. Thus, the problem with experiments, especially low temperature (below ~ 1400 K), is that the H trapping effect is unavoidable. Furthermore, Franfelder experiments are the only ones done also above 1400 K, where trapping effects are less significant. Therefore, our conclusion is still that the migration barrier of 0.25 eV should be used.

3.2. Diffusion coefficient at different pressures

The diffusion coefficient depends on the pressure in the lattice and can be written as:

$$D = D_0 \exp\left(-\frac{E_m + P\Delta V_m}{kT}\right), \quad (3)$$

where ΔV_m is the migration volume at the saddle point [25]. The migration volume can be obtained from the diffusion coefficient

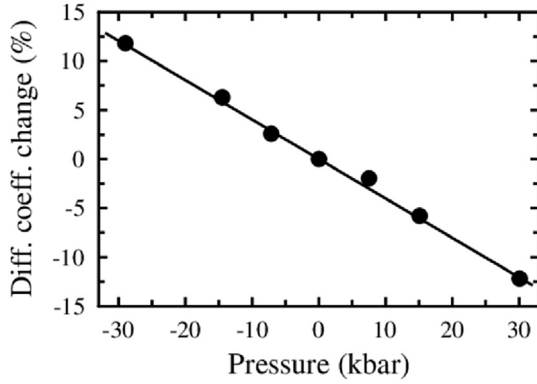


Fig. 3. Change in the simulated D diffusion coefficient as a function of pressure at 900 K. The positive value of the migration volume increases the effective migration barrier, Eq. (4), decreasing the diffusivity at higher pressures.

change at different pressures (T constant)

$$\Delta V_m = -kT \left(\frac{\delta \ln(D)}{\delta P} \right)_T. \quad (4)$$

Fig. 3 shows the change in the D diffusion coefficient at 900 K for different pressures. The calculated migration volume from Eq. (4) is $\Delta V_m \approx 0.488 \text{ \AA}^3$. Higher pressure in the lattice results in lower diffusion coefficient. This effect might become an important factor when high flux He and H from fusion plasma cause high pressure and volumetric swelling in the fusion first wall material.

3.3. Diffusion coefficient at high concentrations

The diffusion coefficient for D atoms with D fractions (D/W ratio) up to about 0.43 is determined. In this case, the Wigner-Seitz cell analysis to find the right tetrahedral interstitial position from MD simulations becomes increasingly ambiguous due to the large lattice distortion induced by the increasing fraction of D atoms. Hence, the Wigner-Seitz cell analysis can not be employed and we use the D positions directly from the MD simulations. Therefore, the distance squared: ΔR_i^2 in Eq. (1) includes also the random oscillation of the D atom around its equilibrium position. This means that when a large number of MD simulations are done, the obtained mean displacement squared is larger than the actual distance squared between two atomic equilibrium positions:

$$\overline{\Delta R_{MD}^2} > \overline{\Delta R^2}, \quad (5)$$

where $\overline{\Delta R_{MD}^2}$ is the simulated mean displacement squared including random oscillation, and $\overline{\Delta R^2}$ is the mean displacement squared (distance squared between two atomic equilibrium positions). This discrepancy gets even more significant when the diffusion path is divided into large number of intervals N (in order to improve statistics). For increasing number of intervals the random oscillation around the equilibrium position becomes comparable to the diffusion path itself, increasing the error for the calculated diffusion coefficient. In the Appendix it is shown that the corrected diffusion coefficient due to random oscillation is

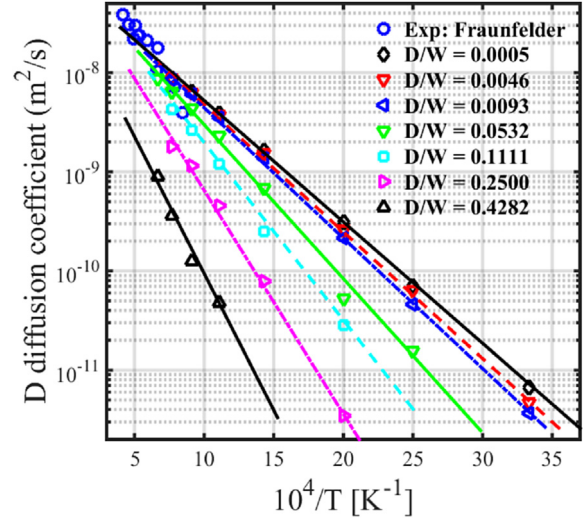


Fig. 4. The simulated D diffusion coefficients as a function of temperature and D/W ratio. The Fraunfelder data (circles) has been divided by square root of D atomic mass, see text. The solid lines are given by Eq. (7).

Table 3

Deuterium diffusion pre-exponential factors (D_0) and migration barriers (E_m) as a function of D/W ratio.

D/W ratio	D_0 (m ² /s)	E_m (eV)
0.0005	0.88×10^{-7}	0.246
0.0046	1.14×10^{-7}	0.269
0.0093	1.14×10^{-7}	0.279
0.0532	0.69×10^{-7}	0.286
0.1111	0.56×10^{-7}	0.308
0.2500	1.05×10^{-7}	0.438
0.4282	0.27×10^{-7}	0.453

$$D = \frac{\sum_i^N \Delta R_{MD,i}^2 - N \times 2\overline{\Delta r^2}}{6\sum_i^N \Delta T}, \quad (6)$$

where $\Delta R_{MD,i}^2$ is the simulated displacement squared and $\overline{\Delta r^2}$ is the mean oscillation distance squared around the atomic equilibrium position. The $\overline{\Delta r^2}$ is obtained from the simulations averaging over thousands of MD simulated position points. By using Eq. (6), we could divide the diffusion path into many intervals (to improve statistics) and still obtain an accurate diffusion coefficient, see Table A.4.

Fig. 4 and Table 3 show how the diffusion coefficient decreases with increasing D/W ratio in the lattice. The D diffusion pre-exponential factors in Table 3 are seen to first increase and then to decrease with increasing D/W ratio, while the migration barrier exhibits a constant increase. The pre-exponential factor should not at any D/W ratio become negative. The following equation for concentration dependent diffusion coefficient obtained in this study, accounts for all these features:

$$D = D_0 \exp\left(-\frac{(X-\alpha)^2}{\beta}\right) \exp\left(-\frac{(E_m + \gamma \cdot X^\delta)}{k_B T}\right), \quad (7)$$

where X is the number of D atoms divided by the total number of interstitial sites: $X = D/(W \cdot 6)$, the BCC lattice has six TIS per atom.

Parameters D_0 , E_m , α , β , γ and δ are the fitting parameters. The – lines in Fig. 4 show that Eq. (7) describes very well the simulated diffusion coefficients for the whole D/W ratio as well as the temperature region. The fitted parameter values are: $D_0 = 1.2737 \times 10^{-7} \text{ m}^2 \text{ s}^{-1}$, $E_m = 0.2430 \text{ eV}$, $\alpha=0.028314$, $\beta=0.002167$, $\gamma=2.13773$ and $\delta=0.73842$. The diffusion coefficient for D starts to deviate significantly from the low concentration limit when the D/W ratio is above 0.01. The observed diffusivity decrease at D/W fractions as low as 0.01 could be explained by the close range repulsive D-D interaction [8,9], where it was seen by Liu et al. [9] that the hydrogen atoms repel each other for distances below about 3.2 Å. This rather long range repulsion will hinder a D atom from diffusing towards another D atom, decreasing the effective diffusion coefficient. This explanation seems feasible, as the observed diffusion coefficient reduction is largest at low temperatures where a small repulsion between atoms is enough to keep them apart.

The decreasing hydrogen diffusion coefficient as a function of H concentration might have serious implications for the properties of tungsten material in hydrogen-rich environments. In high H flux experiments, the concentration of H in W might become much higher than expected due to the self-induced decrease in the diffusivity. This is especially important at low temperatures as seen in Fig. 4, where the diffusivity reduction as a function of concentration is most pronounced.

Experimentally this might have been seen by Alimov et al. [26], where the trapping of deuterium in single crystal W was studied. The irradiation was done at 323 K with D ion energy and flux of 200 eV and $1.9 \times 10^{18} \text{ m}^{-2} \text{ s}^{-1}$, respectively. They observed that a tenfold increase in the ion fluence from $5 \times 10^{22} \text{ D}^+ \text{ m}^{-2}$ to $5 \times 10^{23} \text{ D}^+ \text{ m}^{-2}$ leads to a factor of more than 100 increase in the trapped near-surface D concentration. Their conclusion was that the only explanation to this drastic concentration increase is a sudden structural material change during the irradiation. A reason for this drastic material property change might be the concentration dependent diffusion coefficient; The near-surface solute D concentration will attain a value where the diffusion of D atoms away from the region is the same as the irradiation flux into it. However, if the flux is large enough, the concentration might reach a value where the diffusivity starts to drop. This mobility drop, for a constant incoming D flux, will lead to an increase in the near-surface D concentration. This will further lead to decreasing mobility and so forth, until the D to tungsten atom ratio could be high enough to form a metal hydride system.

4. Conclusions

We have shown how the random oscillation of atoms around the equilibrium position can be dealt with in diffusion simulations. The derived method is general and only the mean oscillation distance squared around the atomic equilibrium position is needed. It improves the accuracy of determining the diffusion coefficient at all temperatures, but the main advantage is that it makes it possible to simulate atomic diffusion, and determine the corresponding diffusion coefficients at lower temperatures than previously.

The results of the present study strongly suggests that the recommended value of 0.39 eV for the H in W migration barrier should be changed to 0.25 eV. This new value agrees very well with the Fraunfelder experiments omitting the two lowest temperature diffusion coefficient points. The effect of introducing the lower migration barrier value in simulations will be most noticeable at low temperatures below about 500 K.

Acknowledgements

This work has been carried out within the framework of the EUROfusion Consortium and has received funding from the Euratom research and training programme 2014–2018 under grant agreement No 633053. The views and opinions expressed herein do not necessarily reflect those of the European Commission. Grants of computer time from the Centre for Scientific Computing in Espoo, Finland, are gratefully acknowledged.

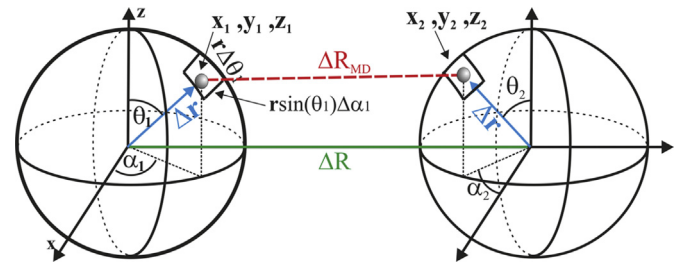
Appendix A. Correction to diffusion coefficient obtained from MD simulations

In MD simulations, the atoms are in constant random oscillation around their equilibrium positions. If the diffusion probability is very small, the random atomic oscillations might cause problems in deducing the right diffusion coefficient from Eq. (1). The problem is illustrated in Fig. A.5, where the right displacement squared (distance squared between two atomic equilibrium positions) for the diffusion is ΔR^2 . But due to the constant atomic oscillation around the equilibrium position, with mean oscillation radius squared $\overline{\Delta r^2}$, the simulated displacement squared ΔR_{MD}^2 can be anything between $(\Delta R - \Delta r)^2$ and $(\Delta R + \Delta r)^2$. When a large number of MD simulations are done, the obtained mean displacement squared will be larger than the actual distance squared between two atomic equilibrium positions

$$\overline{\Delta R_{MD}^2} > \overline{\Delta R^2}. \quad (\text{A.1})$$

This means that the diffusion coefficient calculated from the MD simulations will be overestimated.

Figure A.5: The momentary distance between two atoms ΔR_{MD} , where both atoms are located at a distance Δr from their equilibrium positions. The distance needed to obtain an accurate diffusion coefficient is the distance ΔR between the two equilibrium positions.



To deal with this, we calculate the mean distance squared from all points on the sphere to the left to all points on the sphere to the right. The sphere radius squared is the mean oscillation radius squared: $\overline{\Delta r^2}$. The point x_1, y_1, z_1 on the left sphere, and point x_2, y_2, z_2 on the right sphere are given in spherical coordinates as

$$x_1 = \Delta r \sin(\theta_1) \cos(\alpha_1) \quad x_2 = \Delta r \sin(\theta_2) \cos(\alpha_2) \quad (\text{A.2})$$

$$y_1 = \Delta r \sin(\theta_1) \sin(\alpha_1) \quad y_2 = \Delta r \sin(\theta_2) \sin(\alpha_2) + \Delta R \quad (\text{A.3})$$

$$z_1 = \Delta r \cos(\theta_1) \quad z_2 = \Delta r \cos(\theta_2) \quad (\text{A.4})$$

The distance squared between points on the two spheres is then given as:

$$\begin{aligned} \Delta R_{MD}^2 &= (x_1 - x_2)^2 + (y_1 - y_2)^2 + (z_1 - z_2)^2 = \Delta r^2 \left\{ [\sin(\theta_1) \cos(\alpha_1) - \sin(\theta_2) \cos(\alpha_2)]^2 + \left[\sin(\theta_1) \sin(\alpha_1) - \sin(\theta_2) \sin(\alpha_2) - \frac{\Delta R}{\Delta r} \right]^2 \right. \\ &+ [\cos(\theta_1) - \cos(\theta_2)]^2 \left. \right\} = \Delta r^2 \left\{ \sin^2(\theta_1) \cos^2(\alpha_1) - 2 \sin(\theta_1) \cos(\alpha_1) \sin(\theta_2) \cos(\alpha_2) + \sin^2(\theta_2) \cos^2(\alpha_2) + \sin^2(\theta_1) \sin^2(\alpha_1) \right. \\ &- 2 \sin(\theta_1) \sin(\alpha_1) \sin(\theta_2) \sin(\alpha_2) + 2 \sin(\theta_1) \sin(\alpha_1) \frac{\Delta R}{\Delta r} - 2 \sin(\theta_2) \sin(\alpha_2) \frac{\Delta R}{\Delta r} + \sin^2(\theta_2) \sin^2(\alpha_2) + \frac{\Delta R^2}{\Delta r^2} + \cos^2(\theta_1) \\ &- 2 \cos(\theta_1) \cos(\theta_2) + \cos^2(\theta_2) \left. \right\} = \Delta r^2 \left\{ \sin^2(\theta_1) [\sin^2(\alpha_1) + \cos^2(\alpha_1)] + \sin^2(\theta_2) [\sin^2(\alpha_2) + \cos^2(\alpha_2)] \right. \\ &- 4 \sin(\theta_1) \sin(\alpha_1) \sin(\theta_2) \sin(\alpha_2) + 2 \sin(\theta_1) \sin(\alpha_1) \frac{\Delta R}{\Delta r} - 2 \sin(\theta_2) \sin(\alpha_2) \frac{\Delta R}{\Delta r} + \frac{\Delta R^2}{\Delta r^2} + \cos^2(\theta_1) - 2 \cos(\theta_1) \cos(\theta_2) \\ &+ \cos^2(\theta_2) \left. \right\} = \Delta r^2 \left\{ \sin^2(\theta_1) + \sin^2(\theta_2) - 4 \sin(\theta_1) \cos(\alpha_1) \sin(\theta_2) \cos(\alpha_2) + 2 \sin(\theta_1) \sin(\alpha_1) \frac{\Delta R}{\Delta r} - 2 \sin(\theta_2) \sin(\alpha_2) \frac{\Delta R}{\Delta r} + \frac{\Delta R^2}{\Delta r^2} \right. \\ &+ \cos^2(\theta_1) - 2 \cos(\theta_1) \cos(\theta_2) + \cos^2(\theta_2) \left. \right\} = \Delta r^2 \left\{ 2 - 4 \sin(\theta_1) \cos(\alpha_1) \sin(\theta_2) \cos(\alpha_2) + 2 \sin(\theta_1) \sin(\alpha_1) \frac{\Delta R}{\Delta r} \right. \\ &- 2 \sin(\theta_2) \sin(\alpha_2) \frac{\Delta R}{\Delta r} + \frac{\Delta R^2}{\Delta r^2} - 2 \cos(\theta_1) \cos(\theta_2) \left. \right\} \quad (\text{A.5}) \end{aligned}$$

To get the mean distance squared, we integrate over the two spheres (see Fig. A.5)

$$\overline{\Delta R_{MD}^2} = \frac{1}{16\pi^2} \int_0^\pi \sin(\theta_1) d\theta_1 \int_0^{2\pi} d\alpha_1 \int_0^\pi \sin(\theta_2) d\theta_2 \int_0^{2\pi} d\alpha_2 [\Delta R_{MD}^2] \quad (\text{A.6})$$

which becomes

$$\begin{aligned} \overline{\Delta R_{MD}^2} \frac{16\pi^2}{\Delta r^2} &= 2 \left[\int_0^\pi \sin(\theta_1) d\theta_1 \right] \left[\int_0^{2\pi} d\alpha_1 \right] \left[\int_0^\pi \sin(\theta_2) d\theta_2 \right] \left[\int_0^{2\pi} d\alpha_2 \right] - 4 \left[\int_0^\pi \sin^2(\theta_1) d\theta_1 \right] \left[\int_0^{2\pi} \cos(\alpha_1) d\alpha_1 \right] \left[\int_0^\pi \sin^2(\theta_2) d\theta_2 \right] \\ &\left[\int_0^{2\pi} \cos(\alpha_2) d\alpha_2 \right] + 2 \left[\int_0^\pi \sin^2(\theta_1) d\theta_1 \right] \left[\int_0^{2\pi} \sin(\alpha_1) d\alpha_1 \right] \left[\int_0^\pi \sin(\theta_2) d\theta_2 \right] \left[\int_0^{2\pi} d\alpha_2 \right] \frac{\Delta R}{\Delta r} - 2 \left[\int_0^\pi \sin(\theta_1) d\theta_1 \right] \left[\int_0^{2\pi} d\alpha_1 \right] \\ &\left[\int_0^\pi \sin^2(\theta_2) d\theta_2 \right] \left[\int_0^{2\pi} \sin(\alpha_2) d\alpha_2 \right] \frac{\Delta R}{\Delta r} + \left[\int_0^\pi \sin(\theta_1) d\theta_1 \right] \left[\int_0^{2\pi} d\alpha_1 \right] \left[\int_0^\pi \sin(\theta_2) d\theta_2 \right] \left[\int_0^{2\pi} d\alpha_2 \right] \frac{\Delta R^2}{\Delta r^2} - 2 \left[\int_0^\pi \sin(\theta_1) \cos(\theta_1) d\theta_1 \right] \\ &\left[\int_0^{2\pi} d\alpha_1 \right] \left[\int_0^\pi \sin(\theta_2) \cos(\theta_2) d\theta_2 \right] \left[\int_0^{2\pi} d\alpha_2 \right] \end{aligned}$$

The following integrals: $\int_0^\pi \sin(\theta) d\theta = 2$, $\int_0^\pi \sin^2(\theta) d\theta = \pi/2$, $\int_0^\pi \sin(\theta) \cos(\theta) d\theta = 0$ and $\int_0^{2\pi} \sin(\alpha) d\alpha = \int_0^{2\pi} \cos(\alpha) d\alpha = 0$ finally gives

$$\overline{\Delta R_{MD}^2} = \overline{\Delta R^2} + 2\overline{\Delta r^2}. \quad (\text{A.7})$$

We can thus extract the right distance squared between the atomic equilibrium positions from the MD simulations including the mean random oscillation $\overline{\Delta r^2}$ around equilibrium position as

$$\overline{\Delta R^2} = \overline{\Delta R_{MD}^2} - 2\overline{\Delta r^2} \quad (\text{A.8})$$

The corrected equation for diffusion coefficient with N intervals is then from Eq. (1)

$$D = \frac{\sum_i^N \Delta R_{MD,i}^2 - N \times 2\overline{\Delta r^2}}{6 \sum_i^N \Delta T_i} \quad (\text{A.9})$$

In Table A.4 are shown the errors in the calculated diffusion coefficients for different fractions of atomic random oscillation squared compared to the diffusion distance squared. The errors are deviation from results of Wigner-Seitz cell analysis.

Table A.4. The diffusion coefficient errors for the uncorrected, Eq. (1), and corrected Eq. (A.9) as a function of the random oscillation squared divided by the total diffusion distance squared.

Oscillation around equilibrium position $\overline{\Delta r^2}/\overline{\Delta R_{MD}^2}$ (%)	Uncorrected diffusion coeff. error (%)	Corrected diff. Coeff. error (%)
0.0	0.0	0.0
0.07	0.15	−0.01
0.66	1.33	−0.04
2.53	5.33	0.03
6.45	14.60	−0.20

References

- [1] Y.-N. Liu, X. Shu, Y. Yu, X.-C. Li, Guang-Hong, T. Ahlgren, L. Bukonte, K. Nordlund, Mechanism of vacancy formation induced by hydrogen in tungsten, *AIP Adv.* 3 (12) (2013) 122111.
- [2] W. Wang, J. Roth, S. Lindig, C. Wu, Blister formation of tungsten due to ion bombardment, *J. Nucl. Mater.* 299 (0) (2001) 124–131.
- [3] K. Heinola, T. Ahlgren, K. Nordlund, J. Keinonen, Hydrogen interaction with point defects in tungsten, *Phys. Rev. B* 82 (9) (2010) 094102.
- [4] D. Terentyev, V. Dubinko, A. Bakaev, Y. Zayachuk, W.V. Renterghem, P. Grigorev, Dislocations mediate hydrogen retention in tungsten, *Nucl. Fusion* 54 (4) (2014) 042004.
- [5] H.-B. Zhou, Y.-L. Liu, S. Jin, Y. Zhang, Investigating behaviours of hydrogen in a tungsten grain boundary by first principles: from dissolution and diffusion to a trapping mechanism, *Nucl. Fusion* 50 (2010) 025016.
- [6] R. Frauenfelder, Solution and diffusion of hydrogen in tungsten, *J. Vac. Sci. Technol.* 6 (3) (1969) 388.
- [7] G.E. Murch, R.J. Thorn, Computer simulation of sodium diffusion in β -alumina, *Philos. Mag.* 35 (1977) 493.
- [8] C. Becquart, C. Domain, A density functional theory assessment of the clustering behaviour of He and H in tungsten, *J. Nucl. Mater.* 386–388 (0) (2009) 109–111.
- [9] Y. Liu, Y. Zhang, G. Luo, G. Lu, Structure, stability and diffusion of hydrogen in tungsten: a first-principles study, *J. Nucl. Mater.* 390–391 (2009) 1032–1034.
- [10] K. Nordlund, Molecular dynamics simulation of ion ranges in the 1100 keV energy range, *Comput. Mater. Sci.* 3 (1995) 448.
- [11] X.-C. Li, X. Shu, Y.-N. Liu, F. Gao, G.-H. Lu, Modified analytical interatomic potential for a W system with defects, *J. Nucl. Mater.* 408 (1) (2011) 12.
- [12] C.A. Wert, Diffusion coefficient of C in α -iron, *Phys. Rev.* 79 (1950) 601.
- [13] A.H. Schoen, Correlation and the isotope effect for diffusion in crystalline solids, *Phys. Rev. Lett.* 1 (Aug 1958) 138–140.
- [14] A.T. Macrander, D.N. Seidman, An atomprobe fieldion microscope study of 200eV 1H^+ ions implanted in tungsten at 29 K, *J. Appl. Phys.* 56 (6) (1984) 1623–1629.
- [15] K. Heinola, T. Ahlgren, Diffusion of hydrogen in bcc tungsten studied with first principle calculations, *J. Appl. Phys.* 107 (11) (2010) 113531.
- [16] M.W. Guinan, R.N. Stuart, R.J. Borg, Fully dynamic computer simulation of self-interstitial diffusion in tungsten, *Phys. Rev. B* 15 (1977) 699–710.
- [17] P. Grigorev, D. Terentyev, G. Bonny, E. Zhurkin, G.V. Oost, J. Noterdaeme, Interaction of hydrogen with dislocations in tungsten: an atomistic study, *J. Nucl. Mater.* 465 (2015) 364.
- [18] K. Heinola, T. Ahlgren, First-principles study of H on the reconstructed $w(100)$ surface, *Phys. Rev. B* 81 (7) (2010) 073409.
- [19] V. Nemanic, B. Zajec, D. Dellasega, M. Passoni, Hydrogen permeation through disordered nanostructured tungsten films, *J. Nucl. Mater.* 429 (2012) 92–98.
- [20] R. Causey, T.J. Venhaus, The use of tungsten in fusion reactors: a review of the hydrogen retention and migration properties, *Phys. Scr.* T94 (2001) 9.
- [21] T. Tanabe, Review of hydrogen retention in tungsten, *J. Nucl. Mater.* T159 (2014) 014044.
- [22] T. Ikeda, T. Otsuka, T. Tanabe, Application of tritium tracer technique to determination of hydrogen diffusion coefficients and permeation rate near room temperature for tungsten, *Fusion Sci. Technol.* 60 (2011) 1463.
- [23] H. Jónsson, G. Mills, K. Jacobsen, in: B.J. Berne, G. Ciccotti, D.F. Coker (Eds.), *Nudged Elastic Band Method for Finding Minimum Energy Paths of Transitions*, in *Classical and Quantum Dynamics in Condensed Phase Simulations*, World Scientific, Singapore, 1998, p. 385.
- [24] D. Johnson, E.A. Carter, Hydrogen in tungsten: absorption, diffusion, vacancy trapping, and decohesion, *J. Mater. Res.* 25 (2010) 315.
- [25] R.N. Jefferly, D. Lazarus, Calculating activation volumes and activation energies from diffusion measurements, *J. Appl. Phys.* 41 (7) (1970) 3186–3187.
- [26] V.K. Alimov, J. Roth, Hydrogen isotope retention in plasma-facing materials: review of recent experimental results, *Phys. Scr.* T128 (2007) 6.